Structure, Dynamics, and Insertion of a Chloroplast Targeting Peptide in Mixed Micelles†

Hans L. J. Wienk,*,‡ Rainer W. Wechselberger,§ Michael Czisch,§,|| and Ben de Kruijff‡

Department of Biochemistry of Membranes, Centre of Biomembranes and Lipid Enzymology, Institute of Biomembranes, and Department of NMR Spectroscopy, Bijvoet Center for Biomolecular Research, Utrecht University, Padualaan 8, 3584 CH Utrecht, The Netherlands

Received January 19, 2000; Revised Manuscript Received April 24, 2000

ABSTRACT: Nuclear-encoded, chloroplast-destined proteins are synthesized with transit sequences that contain all information to get them inside the organelle. Different proteins are imported via a general protein import machinery, but their transit sequences do not share amino acid homology. It has been suggested that interactions between transit sequence and chloroplast envelope membrane lipids give rise to recognizable, structural motifs. In this study a detailed investigation of the structural, dynamical, and topological features of an isolated transit peptide associated with mixed micelles is described. The structure of the preferredoxin transit peptide in these micelles was studied by circular dichroism (CD) and multidimensional NMR techniques. CD experiments indicated that the peptide, which is unstructured in aqueous solution, obtained helical structure in the presence of the micelles. By NMR it is shown that the micelles introduced ill-defined helical structures in the transit peptide. Heteronuclear relaxation experiments showed that the whole peptide backbone is very flexible. The least dynamic segments are two N- and C-terminal helical regions flanking an unstructured proline-rich amino acid stretch. Finally, the insertion of the peptide backbone in the hydrophobic interior of the micelle was investigated by use of hydrophobic spin-labels. The combined data result in a model of the transit peptide structure, backbone dynamics, and insertion upon its interaction with mixed micelles.

The majority of chloroplast proteins are synthesized in the plant cell cytosol as precursors. Their N-terminal transit sequences contain all the information that is necessary (*1, 2*) and sufficient (*3*) to recognize the chloroplast and to translocate these precursors across its envelope membranes. Many precursor proteins are imported via one general import route (*4*−*6*), although transit sequences differ greatly in length and do not share amino acid sequence homology (*7*). It has been suggested that in aqueous solution transit sequences are designed to be random coil (*8*) and that they obtain common, recognizable structures after initial interactions with the chloroplast outer membrane. What these motifs are is yet completely unknown. An excellent protein to get insight in this question is the *Silene pratensis* preferredoxin (preFd).[1] Because import of preFd into chloroplast does not require cytosolic factors (*9*), the transit sequence can interact directly with the outer membrane. In previous studies it has been shown that also the isolated preFd transit peptide (trFd), either chemically synthesized (*10*) or isolated from *Escherichia coli* (*11*), is able to interact functionally with the general import machinery. This makes this peptide, which is considerably smaller than the complete precursor, a suitable molecule to study the structural behavior by NMR spectroscopy. Previously, it has been shown that in aqueous solution trFd is in a random coil conformation, while in the hydrophobic solvent trifluoroethanol N- and C-terminal helical structures are introduced (*12*). This illustrates that interaction with the hydrophobic interior of a membrane may introduce structural motifs in transit peptides.

Monolayer studies pointed out that the ferredoxin transit peptide is able to insert into lipids extracted from the chloroplast outer membrane (*13*). In a deletion mutant study (*14*) it was shown that when the N-terminal amino acids

† This work is part of the program Chloroplast Protein Import and was carried out under auspices of the Foundation of Life Sciences (SLW) with financial aid from The Netherlands Foundation for Scientific Research (NWO). Part of this research was supported by a grant in a program between NWO and the Russian Federation (NL-RF 047.006.004). The dynamic light scattering experiments were performed at the Department of Crystal and Structural Chemistry, Utrecht University, The Netherlands. The NMR experiments were acquired at the SON NMR Large Scale Facility, Utrecht, The Netherlands. Support from the European Community for M.C. (Contract ERBFM GECT 950032) is acknowledged.

* To whom correspondence should be addressed: fax (31) (30) 252 2478; e-mail h.l.j.wienk@chem.uu.nl.

‡ Department of Biochemistry of Membranes, Centre of Biomembranes and Lipid Enzymology, Institute of Biomembranes.

§ Department of NMR Spectroscopy, Bijvoet Center for Biomolecular Research.

|| Present address: Max Planck Institute for Psychiatry, AG NMR, Kraepelinstr. 2-10, D-80804, Munich, Germany.

[1] Abbreviations: CD, circular dichroism; DLS, dynamic light scattering; DPC, dodecylphosphocholine; DPG, dodecylphosphoglycol; 5- and 16-DSA, 5- and 16-doxylstearic acid, respectively; HSQC, heteronuclear single quantum coherence spectroscopy; MGDG, monogalactosyldiacylglycerol; NOESY, nuclear Overhauser enhancement spectroscopy; PC, phosphatidylcholine; PG, phosphatidylglycerol; preFd, precursor of the *Silene pratensis* protein ferredoxin; R_h, hydrodynamic radius; TOCSY, total correlation spectroscopy; trFd, 47 amino acid long transit peptide of precursor ferredoxin followed by amino acids Ala48-Ser49-Gly50-Leu51-Pro52.

10.1021/bi000110i CCC: $19.00
Published on Web 06/20/2000

Thr6−Leu14 are deleted from the preFd transit sequence, recognition of chloroplasts is completely abolished. In addition, this mutant showed diminished interaction with isolated outer membrane lipids, in particular with the glycolipid monogalactosyldiacylglycerol (MGDG), which is a chloroplast-specific lipid. This suggests that this part of the transit sequence is involved in a functional interaction with lipids. The transit sequence C-terminus appears also to contain information that improves binding of preFd to isolated chloroplasts. Monolayer experiments showed that C-terminal deletions cause an impaired insertion into chloroplast outer envelope lipids, especially with PG. In vesicle binding studies it was shown that negatively charged lipids are also responsible for transit sequence binding to a bilayer system comparable to the chloroplast outer membrane lipid phase (*15*). These results imply that the trFd N- and C-terminal regions are able to interact with different chloroplast lipids and that these interactions are of functional importance.

By vesicle leakage experiments it was shown that the transit peptide of ribulose-1,5-bisphosphate carboxylase/oxygenase small subunit can cause lipid vesicle leakage when negatively charged lipids and MGDG are present (*16*). This indicates that the interaction between precursor proteins and chloroplast lipids may be of general significance for the import process.

Circular dichroism showed that negatively charged lipids induce some amount of helix in the transit peptide (*17*). This effect was enhanced when MGDG was also present. These results strongly suggest that the same lipids that facilitate insertion into extracted chloroplast outer membrane lipids are simultaneously inducing structural changes in the transit peptide.

Circular dichroism can give information about percentages of secondary structural elements in a protein but does not reveal where structures are present in the protein. Therefore, the aim of this study was to obtain structural information for trFd upon insertion into a lipid system by nuclear magnetic resonance (NMR). Because high-resolution NMR on proteins in lipid vesicles is difficult due to the spectral line broadening caused by the size of a vesicular system, micelles were used as a model system.

Mixed micelles, composed of chloroplast lipids and detergents mimicking chloroplast lipids, were designed to be suitable for NMR analysis. The selected system consisted of MGDG and the detergents dodecylphosphoglycol (DPG) and dodecylphosphocholine (DPC), in a 1:2:97 molar ratio. By NMR it is shown that when trFd interacted with the micelles, N- and C-terminal helical features are introduced and that in the presence of micelles the transit peptide has a very dynamic backbone. The least flexible parts were detected at the end of the N-terminal helical region and in the first part of the C-terminal half of the peptide. In addition, information of the orientation of the transit peptide in the micelle has been obtained by use of hydrophobic spin-labels.

MATERIALS AND METHODS

Materials. Unlabeled and ^{15}N-labeled trFd were isolated as the 47 amino acid long wild-type *Silene pratensis* preferredoxin transit peptide followed by the extension Ala48-Ser49-Gly50-Leu51-Pro52, as described (*11*, *12*). ^{1}H-DPC was purchased from Avanti Polar Lipids, Inc. (Alabaster, AL), ^{2}H-DPC from Isotec, Inc. (Miamisburg, OH), and plant MGDG from Larodan Lipids (Malmö, Sweden). MGDG was judged pure from TLC experiments. Gas chromatography followed by mass spectrometry pointed out that 97% of its methyl-esterified fatty acids were hexadecatrienoic acid (16:3) and linolenic acid (18:3), in a 1:3 molar ratio, which is similar to values described in the literature (*18*). ^{1}H-DPG and ^{2}H-DPG were synthesized essentially according to ref *19*. 5- and 16-Doxylstearic acid (5- and 16-DSA) were obtained from Aldrich Chemical Co. (Milwaukee, WI). The rest of the chemicals used were of the highest grade available.

Sample Preparation. Degassed solvents were used to prepare stock solutions. DPC and MGDG were dissolved in chloroform, and DPG (pK_a = 3.0) was dissolved in chloroform/methanol 1:1 (v/v). Appropriate amounts of detergents and MGDG were mixed, dried under nitrogen, and hydrated in 18 mM KP_i and 0.02% (w/w) sodium azide (with and without trFd, respectively). After thorough vortexing and freeze−thawing and 3 min bath sonication, the samples were filtered five times through a 100 nm filter (Whatman, Maidstone, England) using the ProteinSolutions (Charlottesville, VA) microfilter system.

For spin-label experiments an aliquot of a spin-label stock solution in deuterated methanol was dried by evaporation under nitrogen. Subsequently, a solution of mixed micelles (100 mM lipid) was added to yield a spin-label:lipid ratio of 1:50. The spin-label was incorporated in the micelles by thorough vortexing, followed by a 30 min incubation at 50 °C and a 30 min bath sonication.

Dynamic Light Scattering. Samples containing 100 mM lipid in 18 mM KP_i, pH 4.0, were measured at 20 °C on a ProteinSolutions DynaPro 801 molecular sizing instrument connected to a temperature-controlled microsampler. Data were fitted with the accompanying Dynamics program. The dispersity of the solution was calculated from the difference between measured data and the calculated curve and from values representing the completeness of the autocorrelation function. The calculated hydrodynamic radii are averages of more than 5 values obtained from at least two samples. Control experiments were performed with water, and aqueous solutions of 100 mM octyl β-D-glucopyranoside or 100 mM DPC.

Circular Dichroism. CD spectra were recorded on a Jasco-600 spectropolarimeter at 20 °C, as described (*17*). Data were corrected by subtraction of spectra obtained for peptide-free samples. Micelle-free measurements were performed with 0.1 mM trFd solution in 18 mM KP_i and 0.02% NaN_3, pH 4.0 or pH 7.4, after which micelles were titrated to a final 100 mM lipid concentration. Deconvolution was performed as described (*19*).

NMR Measurements. Peptide samples were measured in 5 mm Shigemi tubes. Structure elucidation was performed with 0.7 mM [^{15}N]trFd in 280 μL of 18 mM KP_i, 0.02% (w/v) sodium azide, 10% (v/v) $^{2}H_2O$, and 100 mM MGDG−^{2}H-DPG−^{2}H-DPC micelles (1:2:97 mol/mol/mol) at pH 4.75 (pH meter reading) and 30 °C. Protons were calibrated on the water signal. ^{15}N chemical shifts were calculated by indirect referencing (*20*).

Three-dimensional (^{15}N,^{1}H) TOCSY−HSQC and NOESY−HSQC (*21*) NMR experiments were performed on a Varian

Unity Inova 750 MHz spectrometer equipped with a triple-resonance gradient probe. Spectral widths were 8000 and 1600 Hz for protons and nitrogen, respectively. Water suppression was achieved by gradient coherence selection of ^{15}N (*22*). Data sets of 240 × 80 × 992 complex points in *t*1 (^{1}H), *t*2 (^{15}N), and *t*3 ($^{1}H^{N}$), respectively, were recorded with States time-proportional phase incrementation (TPPI) (*24*) in *t*1. The NOESY mixing time was 150 ms and the TOCSY experiment was performed with a DIPSI sequence (*23*) with a 50 ms mixing time.

^{15}N{^{1}H} heteronuclear NOE experiments (*24*, *25*) were performed on a Varian Unity Inova 500 MHz spectrometer. Two data sets were recorded with 736 ($^{1}H^{N}$) × 148 (^{15}N) complex points each, one with and one without proton saturation. In these experiments the relative differences in peak intensities have been shown to reflect backbone mobility in a protein (*26*, *27*). States-TPPI was applied in *t*1 (^{15}N). Sweep widths were 6800 Hz in the proton dimension and 1400 Hz for ^{15}N. A relaxation delay of 1.5 s was applied.

The insertion of 5- and 16-DSA was investigated on protonated micelles by 1D proton NMR measurements and ^{13}C NMR experiments with GARP composite-pulse proton decoupling. ^{15}N−^{1}H HSQC (*28*, *29*) spectra were recorded on 0.25 mM [^{15}N]trFd in 100 mM deuterated micelles (with protonated MGDG) on a Varian Unity Inova 500 MHz spectrometer. Data sets of 768 (H^{N}) × 128 (^{15}N) complex points were recorded, with States-TPPI in the nitrogen dimension. Spectral widths were 5000 Hz in the proton dimension and 1400 Hz for nitrogen.

The programs NMRPipe (*30*) and REGINE (*31*) were used for processing and data analysis, respectively. In the ^{15}N dimension a linear prediction was performed. Data were multiplied by a sine bell function in all dimensions followed by zero-filling, Fourier transformation, and baseline corrections. Final 3D data matrixes of 512 × 128 × 1K points were analyzed (*32*). Transit peptide structures were drawn with Molmol (*33*).

RESULTS

Formation of Uniformly Mixed Micelles. To study the structure of trFd in a membrane-lipid mimetic environment by NMR, we decided to use mixed micelles. These were composed of the zwitterionic detergent DPC, which has a headgroup identical to that of PC (an abundant chloroplast outer envelope phospholipid); the negatively charged detergent DPG, to mimic the anionic phospholipid PG; and the galactolipid MGDG, isolated from plant chloroplasts. The incorporation of diacyl lipids such as MGDG in micelles may drastically increase their radius, which might thereby cause line broadening of NMR signals. To study the size and dispersity of the mixed micelles, dynamic light scattering was used. As a control the hydrodynamic radius (R_h) of octyl β-D-glucopyranoside was reproduced (literature value (*34*) R_h = 2.3 ± 0.3 nm; measured R_h = 2.59 ± 0.10 nm). In NMR studies DPC (cmc = 1.5 mM) is often used as a phospholipid-mimicking detergent because it forms sufficiently small micelles (e.g., ref *27*). The radius of the DPC micelles was found to be 2.55 ± 0.12 nm. The three-component system to be designed was aimed to have a radius close to this value. Inclusion of 1 mol % MGDG in the DPC micelles resulted in a R_h of 2.65 ± 0.04 nm. To obtain a ternary system, DPG was titrated. DPG contents of 10 mol % and higher gave rise to micelle polydispersity. Furthermore, the presence of small amounts of DPG already caused a small, though significant, rise in hydrodynamic radius. As a compromise between anionic detergent content and radius of the micelles, 2 mol % DPG was selected for titration with MGDG. However, already above 2 mol % MGDG the micelles were polydisperse. In addition, even a MGDG content of 2 mol % led to an undesirably high R_h value. The results indicate that maximal amounts of 2 mol % DPG and 1 mol % MGDG can be used to maintain a uniformly sized mixed micelle with a hydrodynamic radius (2.78 ± 0.06 nm) that is still acceptable for NMR studies. Addition of trFd to the micelles (1:1000 molar ratio) did not cause an increase in dispersity and resulted in a hydrodynamic radius of 2.66 ± 0.06 nm. The combined data indicate that the developed detergent−lipid−peptide system is suitable for NMR analysis.

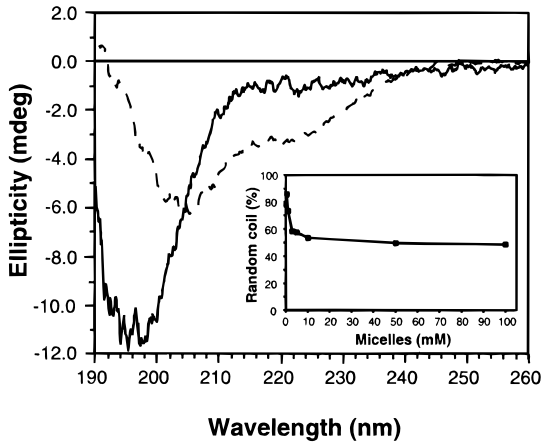

FIGURE 1: CD measurements of 0.1 mM trFd in 18 mM KP_i and 0.02% sodium azide at pH 4 without (solid line) and with (dashed line) 10 mM 1 mol % MGDG/2 mol % DPG/DPC micelles at 20 °C. Inset: Percentages of random coil in trFd upon micelle titration after deconvolution.

Structural Transition of trFd upon Interaction with Mixed Micelles. CD experiments confirmed that in aqueous solution trFd is mainly in a random coil conformation, as indicated by the minimum at 198 nm (Figure 1). Addition of the mixed micelles gave rise to spectral changes. The minima at 205 and 222 nm demonstrate the induction of helical structure. These experiments were performed at pH 4.0, because NMR measurements were intended to be carried out at low pH. To see whether the observed structural change at pH 4.0 also occurs at physiological pH the experiments were repeated at pH 7.4. The results revealed a similar random coil to helix transition as at pH 4.0. The structural changes at pH 4.0 appeared to saturate at a concentration of about 10 mM lipid (Figure 1, inset). This implies that maximal peptide association is achieved when 1 peptide molecule interacts with 100 lipid molecules.

Structure of the Transit Peptide Interacting with Mixed Micelles. The structure of trFd in the presence of mixed micelles was studied by NMR. In the NMR experiments the transit peptide to lipid molar ratio was 1:150, at which maximal trFd association can be expected. Initial ^{15}N−^{1}H HSQC and 1D ^{1}H NMR experiments at different temperatures indicated that up to 30 °C the signal-to-noise ratio for the backbone H^{N}s increased without chemical shift changes (data not shown). This shows that at elevated temperatures

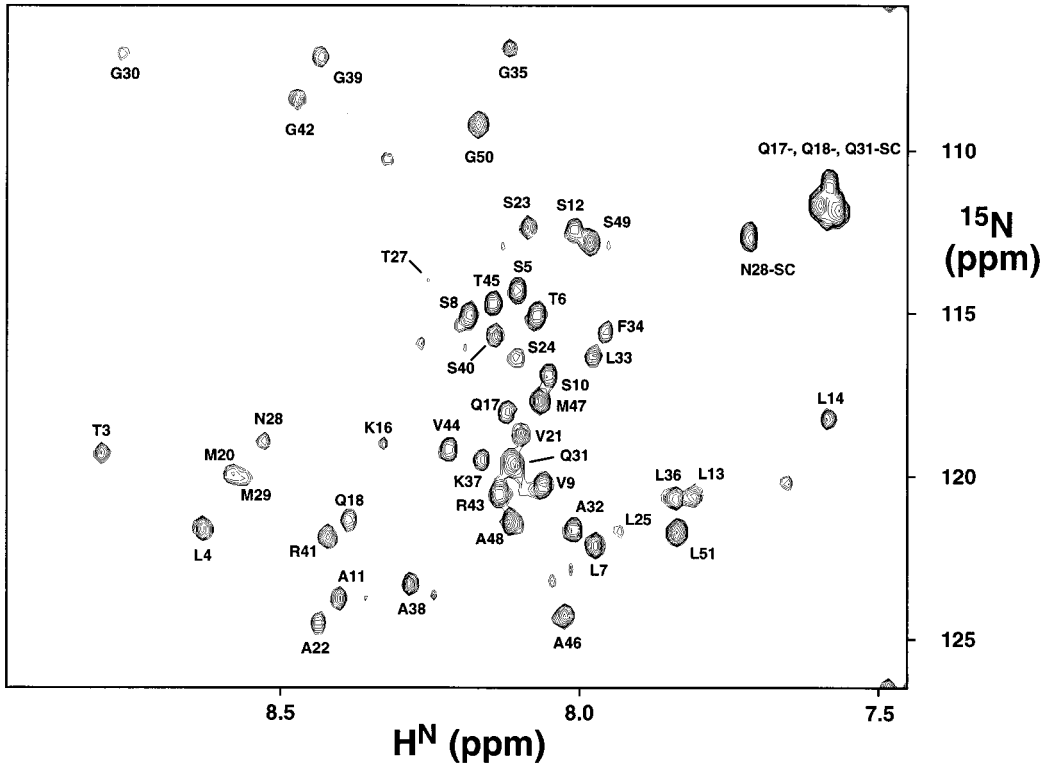

FIGURE 2: Assignment of the peaks in the $^{15}N-^{1}H$ HSQC projection of the 3D $^{15}N-^{1}H$ HSQC−NOESY spectrum of ^{15}N-labeled trFd in 1 mol % MGDG/2 mol % DPG/DPC micelles at 30 °C. SC indicates Asn and Gln side-chain H^N atoms.

the transit peptide structure does not change (which was confirmed by circular dichroism, data not shown), whereas the spectral dispersion had increased, due to overall narrower lines.

For the structural assignment 3D NOESY− and TOCSY−HSQC experiments were performed at 30 °C. The $^{15}N-^{1}H$ HSQC projection of the 3D NOESY−HSQC experiment is presented in Figure 2. Perpendicular to each H^N peak in the HSQC projections, TOCSY and NOESY strips were isolated. A sequential assignment was performed with the NOESY *d*NN, *d*αN, and *dβ*N contacts (Figure 2). Ala1 and Ser2 H^N cross-peaks were not detected, probably due to fast proton exchange at the extreme N-terminus. Although many peaks in the HSQC projection could be assigned, a number of peaks also were present that could not be assigned. This could mean that (part of) the peptide undergoes slow conformational changes. No further information about these peaks was obtained.

For long-chain amino acids not all side-chain protons were observed. Interresidue NOE volumes were estimated and categorized into five intensity groups and are summarized in Figure 3A. Secondary structure information can be obtained from the *d*NN to *d*αN ratio as well as from the presence and intensity of medium-range NOEs. The absence of peaks and relatively low *d*NN intensities indicate extreme flexibility in the N-terminal four residues. Toward Pro15 the peptide might become more structured as suggested by the decrease in *d*αN intensity. Furthermore, the presence of the *d*NN(i, $i + 2$) cross-peak is indicative of helix formation and the presence of the *d*αN(i, $i + 2$) contact suggests an initial helical structure (*35)*. In this trFd segment some of the observed cross-peaks could not be assigned unambiguously due to extensive spectral overlap. In the stretch between Gln17 and Pro26 only two medium-range contacts are observed, indicating the absence of regular secondary structure elements. Toward Leu51 many clues for helical structure can be found, like *d*NN(i, $i + 2$), *d*αN(i, $i + 3$), and *d*αN(i, $i + 4$) connectivities. The latter indicates the presence of an α-helix winding from Gly30 to Phe34. There is a relatively strong *d*αN(i, $i + 2$) NOE between Ala38 and Ser40. Together with the weak *d*NN and strong *d*αN, this suggests that this helical part of trFd is interrupted. The *d*αN-(i, $i + 2$) contacts around Thr27 and Gly50 indicate that toward the termini this region becomes less structured. For the complete peptide no long-range NOEs could be assigned, suggesting that no tertiary structure elements are induced in trFd by the micelles.

Another source of information about secondary structure elements of a protein results from observed H^{α} proton chemical shifts when these are compared with random coil values (*36*). Three adjacent amino acids showing downfield changes (positive values) of more than 0.1 ppm indicate the presence of a stable *β*-structure, while three residues with negative changes over 0.1 ppm point to a well-defined helical structure. Figure 3B shows that many disparities from random coil values are observed but no extended secondary structures are found. Leu14, Leu25, and Leu51 all precede prolines, from which it is known that they can cause artifacts in this kind of data analysis. This complicated the identification of the secondary structure for the region between Leu13 and Pro26 by this method. Helical structures are most pronounced between Ser10 and Ser12, Met29 and Phe34, and Thr45 and Ser49.

Backbone Dynamics of trFd Inserted into Mixed Micelles. The measurement of heteronuclear NOEs has been shown to give detailed information about backbone dynamics (*26*, *27*). In Figure 4 the calculated NOE values (*26*) are displayed for each amino acid residue. From the magnitudes of the

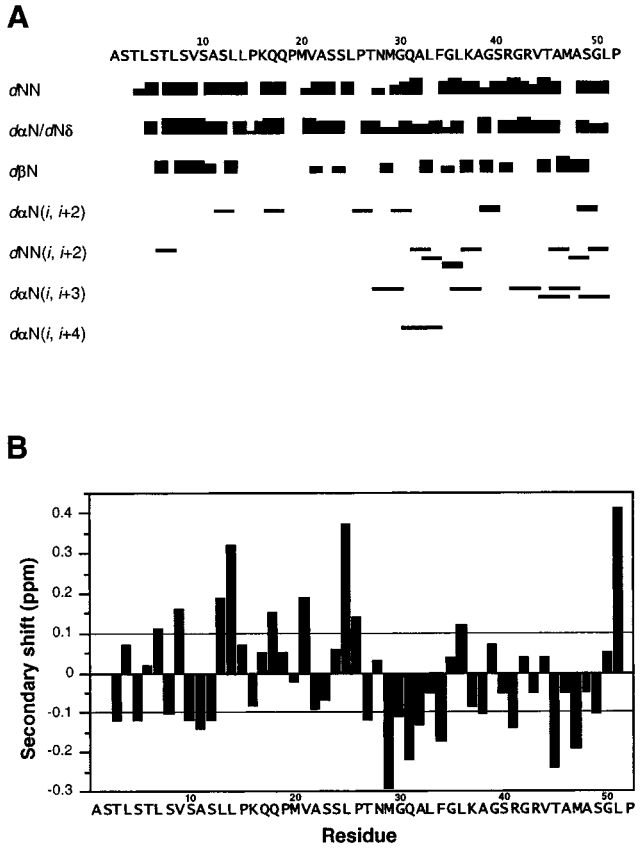

FIGURE 3: Secondary structure determination of ^{15}N-labeled trFd in mixed micelles. (A) Summary of all interresidue NOEs (the NOESY mixing time was 150 ms). The height of the bars is an indication for the relative volume of the observed NOE. For prolines the *d*N*δ* contacts are included in the *d*α N row. (B) Secondary shift calculations: the difference between measured values and temperature corrected random coil values of the H^{α} chemical shift is calculated for each amino acid.

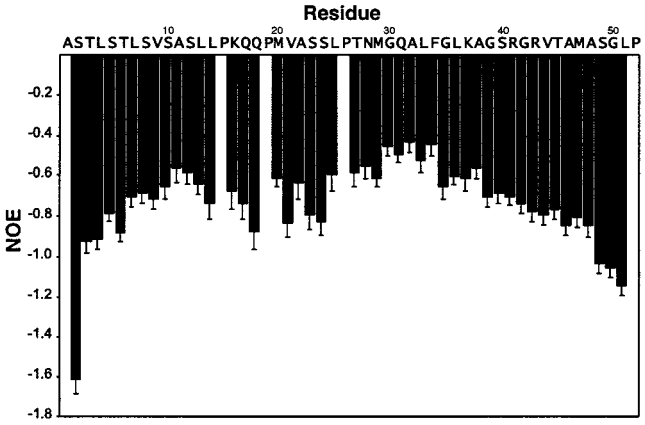

FIGURE 4: ^{15}N{^{1}H} heteronuclear NOE values of backbone amide protons for ^{15}N-labeled trFd in mixed micelles.

values, which are roughly distributed between −0.4 and −0.8, it is concluded that the complete peptide is flexible (*26*). Therefore, the helical structures that were indicated from the CD measurements (Figure 1), the summarized proton NOEs, and the calculated secondary shifts (Figure 3) are dynamic. The helical parts flanking the unstructured and highly mobile region Pro15−Pro26 appear to form the most rigid structures in the peptide. From these segments toward the N- and C-termini the flexibility of the trFd backbone gradually increases. This indicates that the putative C-terminal helical structures exhibit increasing backbone dynamics.

Insertion of trFd in Mixed Micelles. Insertion of 5- and 16-DSA in the mixed micelle was studied with 1D proton and ^{13}C NMR measurements on micelles containing protonated compounds. From DPC peak line broadening and intensity decreases it was concluded that both spin labels insert into the hydrophobic interior of the micelle (data not shown). The doxyl group of 16-DSA was located mostly around the micelle center, whereas the spin-label effect of 5-DSA was observed predominantly at the hydrophobic side of the DPC phosphate group.

The insertion of trFd amino acids in the hydrophobic interior of the micelle was measured by the decrease in amide proton peak intensity upon the presence of 5- or 16-doxylstearic acid. In Figure 5, ^{15}N−^{1}H HSQC spectra without (A) and with 5-DSA (B) and 16-DSA (C) are displayed with similar noise levels. The fact that most of the assigned peaks are affected by the presence of the spin labels indicates that the peptide structure described above is for trFd associated with the micelle and that most of the peptide backbone is either permanently inserted into or able to interact with the hydrophobic interior of the micelle. The results obtained for 5- and 16-DSA were combined after which backbone amide protons were categorized in three groups. Group I consists of H^{N}s that are present in the hydrophobic interior of the micelle. Group II contains amide protons that insert into the headgroup region or interface of the micelle. Peaks that are hardly influenced by the presence of the spin-label are representative of H^{N}s of amino acids that do not enter the micelle (group III). The group distribution of trFd is displayed in Figure 5D. Along the N-terminal region, up to Ser12, amide protons can be found in either hydrophilic or hydrophobic environments. This suggests that this part of trFd is located in the interface of the micelle, parallel to the micelle surface, with some residues in the micelle interior and some in aqueous solution. The following region, essentially from Leu13 to Leu25, contains amino acids that are located in the hydrophobic core of the micelle. The beginning of the C-terminal half of trFds is probably located at the micelle interface. From Leu33 to Ser40 a more hydrophobic environment is preferred. Toward the C-terminus trFd appears to be in a more hydrophilic environment. This region of the peptide may be bound to the micelle by Val44, Ala46, and Met47. The positions of the extreme N- and C-termini were not determined by this method. Ala1 is positively charged and might therefore prefer a hydrophilic environment, but it might also interact with the phosphate groups of the negatively charged detergent, which are located in the micelle interface. The C-terminal proline of the peptide is negatively charged and is probably repulsed by the negatively charged micelle, thus remaining in an aqueous environment.

The presence of undeuterated MGDG allows one to investigate putative specific trFd-lipid interactions by proton NMR techniques. Contacts are indicated by NOEs between trFd and MGDG or by changes in chemical shifts of MGDG protons. Direct NOEs, however, could not be assigned. Furthermore, changes in MGDG proton chemical shifts were not conclusive because of overlap with water and peptide peaks (data not shown). Therefore, no information about parts of trFd and MGDG interacting with each other was obtained.

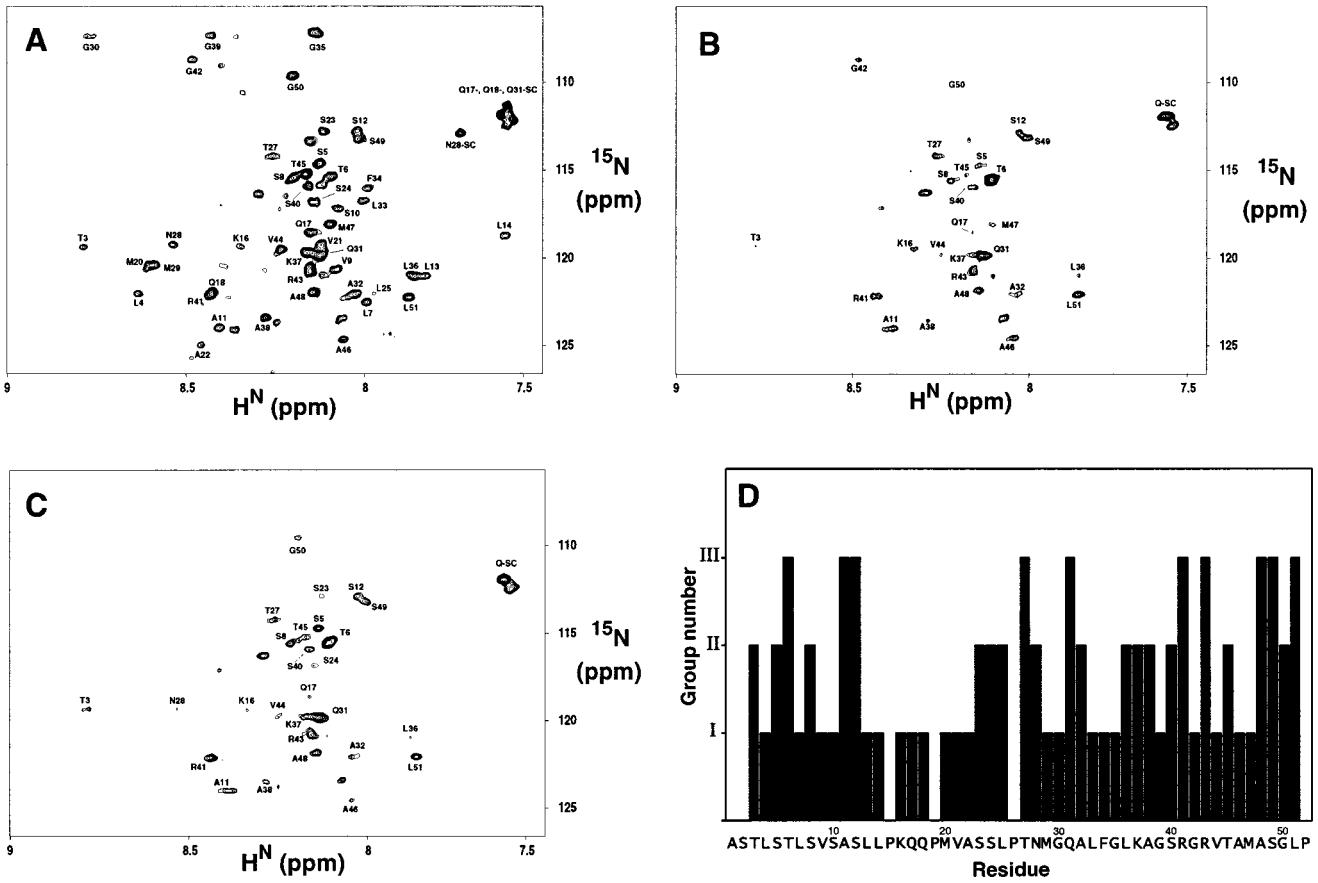

FIGURE 5: ^{1}H−^{15}N HSQCs of ^{15}N-labeled trFd in 100 mM mixed micelles in the absence (A) or presence (B) of 2 mM 5-doxylstearic acid or the presence (C) of 2 mM 16-doxylstearic acid. (D) Results for 16-DSA are combined with data obtained for 5-DSA. Backbone amide proton peaks from the HSQCs are categorized into three groups: I: located in the micelle interior; II, located in the interface region; and III, located outside the micelle.

DISCUSSION

System Characterization. The aim of this study was to get structural information for the preferredoxin transit peptide in a micelle system containing chloroplast membrane lipids and detergents that mimic chloroplast lipids. The micelles were designed to be composed of a matrix of a zwitterionic detergent to mimic the abundant zwitterionic lipid PC, a negatively charged detergent to mimic the negatively charged lipid PG, and small amounts of plant MGDG. It is described that the optimized three-component lipid mixture (in which the molar ratio MGDG/DPG/DPC is 1/2/97) is monodisperse with a hydrodynamic radius similar to that of DPC, which is often used to study the structure of membrane-active peptides by NMR (e.g., refs *27* and *37*). Negatively charged lipids and MGDG were introduced because it has been shown before that these amphiphiles cause structural changes in trFd (*17*). Although MGDG is a diacyl lipid, both from the dynamic light scattering data and the spectral resolution of MGDG observed by NMR it can be concluded that in small amounts it can be incorporated in the micelles. Dynamic light scattering also pointed out that the presence of the transit peptide did not increase the dispersity, indicating an overall uniform mixture. CD measurements showed that the mixed micelles introduce helical structures in the otherwise unstructured transit peptide at low as well as at physiological pH. The CD deconvolution values obtained resemble those observed previously for the chemically synthesized preFd transit peptide interacting with a bilayer system consisting of the three lipids dioleoyl-PC, dioleoyl-PG, and MGDG (*17*). This indicates that the structural features of trFd that are observed in the presence of the mixed micelles can represent the structures induced in trFd upon interaction with chloroplast lipids.

Structural Features of trFd. Different aspects of the interaction between trFd and the mixed micelles were studied by NMR spectroscopy. The secondary structure of the peptide was elucidated, information about backbone dynamics was obtained, and also the topology of the peptide with respect to the micelle interior was determined. Summarizing, trFd has a limited amount of helical structure, it has a highly dynamical backbone, and it is mostly localized in the micelle interface. The combined data result in a model for trFd in the chloroplast membrane, which is shown in Figure 6. The displayed trFd structure was obtained by adapting the backbone ϕ and ψ angles to fit all NMR results. Since no side chain information was obtained they are not presented in the model. This model will be discussed in more detail below.

On the basis of the NMR data several structural regions of the transit peptide can be distinguished. Up to Leu13 some helical features were observed, but mostly these were not conclusive. The NOE data and the secondary shift data did agree upon the presence of helical features between Ser10 and Leu13. When this complete N-terminal segment is drawn

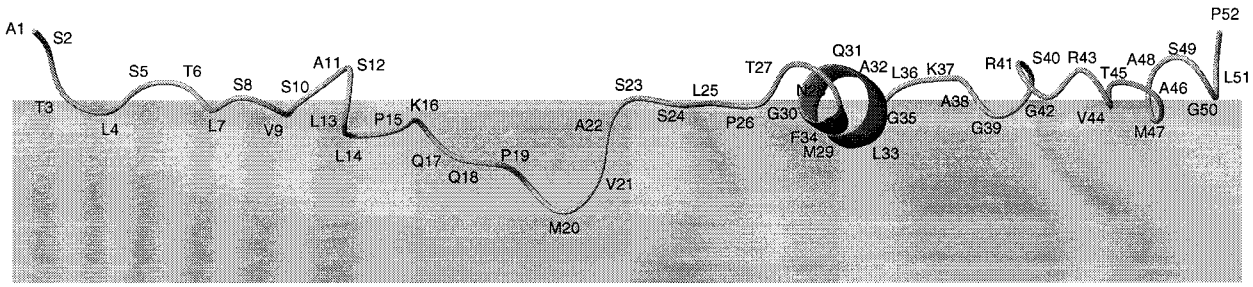

FIGURE 6: Possible trFd secondary structure. Backbone ϕ and ψ angles were varied to fit all NMR data. No side chain information was obtained; therefore side chains are not shown. The most stable helical part is accentuated. The hydrophobic interior of a membrane is displayed in gray.

as a rigid α-helix, the theoretical insertion of this helix in the micelle cannot be brought in accordance with the observed insertion data. By use of the heteronuclear NOE data, which indicated that the helical features become gradually more pronounced toward the start of this region, the backbone insertion data can be fitted. Deep insertion of the N-terminal region into the interior of the micelle is possibly prevented by Ala1 and Lys16, positively charged residues that generally prefer a hydrophilic environment, thus keeping this segment in a topology near the micelle surface. Also Ser12, which is found at the micelle exterior, may contribute to this effect. Although this transit peptide part does not form a stable, general secondary structure element in the micelle, it appears to be amphipathic, with hydroxylated amino acids in a rather hydrophilic environment and hydrophobic residues in a more hydrophobic phase.

TrFd is mostly devoid of structure from Pro15 to Pro26. Hardly any medium-range NOEs were detected and also the secondary shift data suggest that this region is probably designated to be unstructured. The heteronuclear NOE experiment implies that toward the center of this trFd segment the backbone dynamics increases, and that it is bordered by the parts of the peptide that are least dynamical (i.e., Ser10−Leu13 and Gly30−Phe34). The spin-label experiments indicate that this transit peptide domain is able to reside completely in the hydrophobic interior of the micelle. Maybe this region is forced to insert into the lipid hydrophobic phase when it is bound to the micelle interface by the flanking, surface-located, more helical regions.

Between Thr27 and Ser49 the NOE and secondary shift data indicate helical characteristics**,** disrupted between Gly35 and Arg41. This transit peptide region contains the most stable helical element of trFd (Gly30−Phe34). The stability of this structure, however, is still quite low when compared to completely folded proteins (*26*) and, furthermore, the backbone dynamics increases rapidly toward the C-terminus of the peptide. Up to Phe34 this region is found mostly embedded in the hydrophobic interior of the micelle and appears to be bound to the exterior of the micelle by Thr27 and Gln31. The peptide reaches the surface around the unstructured region and the following segment, exhibiting helical features, is attached to the micelle hydrophobic interior only via the side chains of Val44, Ala46, and Met47.

It is of interest to compare current trFd structure with the structure of trFd in aqueous solution, which has been published previously (*12*). The authors described that no structural assignment for trFd in aqueous solution was possible at room temperature. Due to peptide flexibility no H^Ns were observed and, consequently, no backbone assignment could be made. At 5 °C structural assignment was possible. The peptide, though still unstructured, exhibited some tendency toward helix formation. The regions that are most prone to helix formation in aqueous solution are Ser10−Ser12 and Gln31−Gly35. Strikingly, those regions correspond with the most stable structures of trFd in interaction with the mixed micelles. This implies that the micelles magnify intrinsic structural propensities of the transit peptide.

Implications for Transit Peptide Functioning. It has been suggested that the trFd N-terminal 14 residues form a functional domain that is involved in chloroplast recognition via binding to MGDG (*14*). Although it can be envisaged that the interaction between the N-terminus and a hydrophobic/hydrophilic interface can result in the amphipathic segment described, from our data it cannot be concluded that the observed structure in this region is the result of a direct interaction with MGDG. Since an enrichment in the hydroxylated amino acids Ser and Thr is a general feature for chloroplast transit sequences (*7*), the formation of an amphipathic structure or the insertion of such a region in the chloroplast outer membrane may form a general recognition motif for all chloroplast-destined precursor proteins. It would be interesting to see whether the C-terminus of the transit peptide of the small subunit of ribulose-1,5-bisphosphate carboxylase/oxygenase, which has been shown to be able to interact with MGDG and contains several hydroxylated residues (*16*, *38*), also forms such an amphipathic structure.

It was suggested that the region from Pro15 to Leu25 forms a trFd unit that is either required for recognition at later stages of the precursor import process or forms an important flexible linker between other functional regions (*14*). Such a recognition motif could be an unstructured transit sequence region in a hydrophobic environment, which is correctly positioned by N- and C-terminal flanking regions in the membrane interface. The observed lack of structure and high backbone dynamics, however, are also in good agreement with a linker function of this trFd region.

In the C-terminal half of the peptide the region from Pro26 to Ala38 contains the semiconserved FGLK motif. In vitro functionality experiments could not reveal the function of this region (*14*), but it was suggested that it may contribute to targeting. Current NMR results indicate that this region contains the most stable structure, preferably located in a rather hydrophobic environment. Maybe the structural behavior of this region causes correct positioning of a recognition motif in the chloroplast membrane. The trFd region

Leu35−Met47 was suggested to influence import efficiency by stable anchoring of the incoming precursor to the chloroplast by means of electrostatic interactions (*14*). These interactions may drive the insertion of adjacent preFd-parts into the chloroplast envelope so that these can obtain their functional structures and positions in the membrane interface.

When NMR data obtained for trFd are compared with those for other targeting signals, some common characteristics for targeting sequences can be observed. It appears that in aqueous solution all targeting peptides are unstructured, whereas they become (partially) structured, usually helical, in a more hydrophobic environment or in a system with a hydrophobic/hydrophilic interface. Also amphipathic structures have been found before. Targeting peptides from mitochondrial organelles, for instance (e.g., *37*, *39*), form helical structures, which are positively charged on one face of the helix and are enriched in hydrophobic residues on the opposite side. However, many structural differences can also be found between the trFd structure and structures of other targeting peptides. First, although amphipathicity has been observed before for targeting sequences, this is the first time an amphipathic region is found that is enriched in hydroxylated amino acid side chains instead of positively charged residues. In addition, the helical structures in trFd are less pronounced than those detected in other targeting peptides (e.g., *40*, *41*). Finally, many targeting sequences contain helix-disrupting regions. Usually this consists of only one or two glycine or proline residues (e.g., refs *40* and *42*), but in trFd two unstructured, larger regions can be found. The first region comprises amino acids Pro15−Pro26 and contains three proline residues. The other unstructured region (Gly35−Arg41) disturbs the helical features in the C-terminal half of trFd. It contains two glycine residues and is positively charged (Lys36 and Arg41).

The interaction between the transit peptide and the mixed micelles gives rise to some striking structural features but does not result in stable, regular secondary structures. Also the peptide shows very high backbone dynamics. Maybe Von Heijne and Nishikawa (*8*) were right when they postulated that chloroplast transit sequences are designed to be devoid of regular secondary or tertiary structures. However, current NMR results indicate that other structural phenomena in the transit sequence may be introduced when trFd resides in a hydrophobic/hydrophilic interface. These include the induction of an amphiphilic region with opposite hydoxylated and hydrophobic residues, insertion depth of residues of the uncharged N-terminus in the hydrophobic phase, and insertion and positioning of an unstructured, highly mobile region of the transit peptide into a hydrophobic environment. To establish the generality of such motifs it will be necessary to get insight into the structures of more chloroplast transit sequences.

ACKNOWLEDGMENT

We thank G. van Zadelhoff (Department of Bio-Organic Chemistry, Utrecht University) for performing the GC-MS measurements and his help with their interpretation. V. Chupin is thanked for synthesis of the DPG-detergents and for valuable discussions.

SUPPORTING INFORMATION AVAILABLE

One table containing the chemical shift values for trFd ^{15}N and ^{1}H. This material is available free of charge via the Internet at http://pubs.acs.org.

REFERENCES

1. Reiss, B., Wasmann, C. C., and Bohnert, H. J. (1987) *Mol. Gen. Genet. 209*, 116−121.
2. Smeekens, S., Geerts, D., Bauerle, C., and Weisbeek, P. (1989) *Mol. Gen. Genet. 216*, 178−182.
3. Van den Broeck, G., Timko, M. P., Kausch, A. P., Cashmore, A. R., Van Montagu, M., and Herrera-Estrella, L. (1985) *Nature 313*, 358−363.
4. Perry, S. E., Buvinger, W. E., Bennett, J., and Keegstra, K. (1991) *J. Biol. Chem. 266*, 11882−11889.
5. Schnell, D. J., Blobel, G., and Pain, D. (1991) *J. Biol. Chem. 266*, 3335−3342.
6. Cline, K., Henry, R., Li, C. J., and Yuan, J. G. (1993) *EMBO J. 12*, 4105−4114.
7. Von Heijne, G., Steppuhn, J., and Herrmann, R. G. (1989) *Eur. J. Biochem. 180*, 535−545.
8. Von Heijne, G., and Nishikawa, K. (1991) *FEBS Lett. 278*, 1−3.
9. Pilon, M., De Kruijff, B., and Weisbeek, P. J. (1992) *J. Biol. Chem. 267*, 2548−2556.
10. Van 't Hof, R., and De Kruijff, B. (1995) *J. Biol. Chem. 270*, 22368−22373.
11. Wienk, H. L. J., and De Kruijff, B. (1999) *Protein Expression Purif. 17*, 345−350.
12. Wienk, H. L. J., Czisch, M., and De Kruijff, B. (1999) *FEBS Lett. 453*, 318−326.
13. Van 't Hof, R., Van Klompenburg, W., Pilon, M., Kozubek, A., De Korte-Kool, G., Demel, R. A., Weisbeek, P. J., and De Kruijff, B. (1993) *J. Biol. Chem. 268*, 4037−4042.
14. Pilon, M., Wienk, H., Sips, W., De Swaaf, M., Talboom, I., Van 't Hof, R., De Korte-Kool, G., Demel, R., Weisbeek, P., and De Kruijff, B. (1995) *J. Biol. Chem. 270*, 3882−3893.
15. Van 't Hof, R., and De Kruijff, B. (1995) *FEBS Lett. 361*, 35−40.
16. Pinnaduwage, P., and Bruce, B. D. (1996) *J. Biol. Chem. 271*, 32907−32915.
17. Horniak, L., Pilon, M., Van 't Hof, R., and De Kruijff, B. (1993) *FEBS Lett. 334*, 241−246.
18. Billecocq, A. (1974) *Biochim. Biophys. Acta 352*, 245−251.
19. De Jongh, H. H. J., and De Kruijff, B. (1990) *Biochim. Biophys. Acta 1029*, 105−112.
20. Wishart, D. S., Bigam, C. G., Yao, J., Abildgaard, F., Dyson, H. J., Oldfield, E., Markley, J. L., and Sykes, B. (1995) *J. Biomol. NMR 6*, 135−140.
21. Marion, D., Driscoll, P. C., Kay, L. E., Wingfield, P. T., Bax, A., Gronenborn, A. M., and Clore, G. M. (1989) *Biochemistry 28*, 6150−6156.
22. Hurd, R. E., and John, B. K. (1991) *J. Magn. Reson. 91*, 648−653.
23. Shaka, A. J., Lee, C. J., and Pines, A. (1988) *J. Magn. Reson. 77*, 274−293.
24. Abragam, A. (1961) in *The Principles of Nuclear Magnetism*, Clarendon Press, Oxford, England.
25. Dayie, K. T., and Wagner, G. (1994) *J. Magn. Reson. A111*, 121−126.
26. Mulder, F. A. A., Schipper, D., Bott, R., and Boelens, R. (1999) *J. Mol. Biol. 292*, 111−123.
27. Papavoine, C. H. M., Remerowski, M. L., Horstink, L. M., Konings, R. N. H., Hilbers, C. W., and Van de Ven, F. J. M. (1997) *Biochemistry 36*, 4015−4026.
28. Bodenhausen, G., and Ruben, D. J. (1980) *Chem. Phys. Lett. 69*, 185−189.
29. Kay, L. E., Keifer, P., and Saarinen, T. (1992) *J. Am. Chem. Soc. 114*, 10663−10665.

30. Delaglio, F., Grzesiek, S., Vuister, G. W., Zhu, G., Pfeifer, J., and Bax, A. (1995) *J. Biomol. NMR 6*, 277−293.
31. Kleywegt, G. J., Vuister, G. W., Padilla, A., Knegtel, R. M. A., Boelens, R., and Kaptein, R. (1993) *J. Magn. Reson., Ser. B 102*, 166−176.
32. Wüthrich, K. (1986) *NMR of Proteins and Nucleic Acids*, Wiley, New York.
33. Koradi, R., Billeter, M., and Wüthrich, K. (1996) *J. Mol. Graphics 14*, 51−55.
34. Lorber, B., Bishop, J. B., and De Lucas, L. J. (1990) *Biochim. Biophys. Acta 1023*, 254−265.
35. Dyson, H. J., Rance, M., Houghten, R. A., Wright, P. E., and Lerner, R. A. (1988) *J. Mol. Biol. 201*, 201−217
36. Wishart, D. S., and Sykes, B. D. (1994) *Methods Enzymol. 239*, 363−392.
37. Chupin, V., Leenhouts, J. M., De Kroon, A. I. P. M., and De Kruijff, B. (1995) *FEBS Lett. 373*, 239−244.
38. Van 't Hof, R., Demel, R. A., Keegstra, K., and De Kruijff, B. (1991) *FEBS Lett. 291*, 350−354.
39. Bruch, M. D., and Hoyt, D. W. (1992) *Biochim. Biophys. Acta 1159*, 81−93.
40. Chupin, V., Killian, J. A., Breg, J., De Jongh, H. H. J., Boelens, R., Kaptein, R., and De Kruijff, B. (1995) *Biochemistry 34*, 11617−11624.
41. Jarvis, J. A., Ryan, M. T., Hoogenraad, N. J., Craik, D. J., and Høj, P. B. (1995) *J. Biol. Chem. 270*, 1323−1331.
42. Karslake, C., Piotto, M. E., Pak, Y. K., Weiner, H., and Gorenstein, D. G. (1990) *Biochemistry 29*, 9872−9878.

BI000110I